

Lecture Notes for Astronomy 321, W 2004

R. Frey

1 Stellar Energy Generation – Physics background

1.1 Relevant relativity synopsis

We start with a review of some basic relations from special relativity.

The mechanical energy E of a particle of rest mass m moving at speed v , not including any potential energy, is

$$E = \gamma mc^2 ,$$

where

$$\gamma = \frac{1}{\sqrt{1 - (v^2/c^2)}} ,$$

or alternatively

$$E^2 = p^2 c^2 + m^2 c^4$$

where p is the momentum $p = \gamma mv$. The particle rest energy is mc^2 and its kinetic energy is

$$K = E - mc^2 = (\gamma - 1)mc^2 .$$

In the non-relativistic limit, $v \ll c$, we can use the binomial theorem (Taylor series) to expand γ in powers of $(v/c)^2$:

$$\gamma = 1 + \frac{1}{2} \frac{v^2}{c^2} + \frac{3}{8} \frac{v^4}{c^4} + \dots$$

In this limit ($v \ll c$), the kinetic energy reduces to the familiar classical form:

$$K \approx mc^2 \left(1 - 1 + \frac{1}{2} \frac{v^2}{c^2} \right) = \frac{1}{2} mv^2 = p^2/2m$$

We primarily will use the notion of energy-mass equivalence from relativity, since the kinetic energy of protons in main-sequence (MS) stellar cores is typically very small compared to the rest energy. Hence, the non-relativistic

expressions for K are accurate, and we will often notationally use E to mean kinetic energy.

We will borrow the unit system which is customary in atomic, nuclear, and particle physics. Energy is expressed in units of eV, where

$$1 \text{ eV} = 1.60 \times 10^{-19} \text{ J} = 1.60 \times 10^{-12} \text{ erg} .$$

Most importantly, we use $E^2 = p^2c^2 + m^2c^4$ to allow us to also write rest mass and momentum using the eV. So rest mass has units eV/ c^2 (more typically MeV/ c^2), and momentum eV/ c . In this way, we do not usually have to multiply or divide by the numerical value for c .

1.2 Physical data and conversions

$$c = 2.9979 \times 10^8 \text{ m/s}$$

$$1 \text{ eV} = 1.60 \times 10^{-19} \text{ J} = 1.60 \times 10^{-12} \text{ erg}$$

$$1 \text{ fm} = 10^{-15} \text{ m}$$

$$\hbar = h/2\pi = 1.054 \times 10^{-34} \text{ J s} = 6.58 \times 10^{-22} \text{ MeV s}$$

$$\hbar c = 197 \text{ MeV fm}$$

$$e = 1.60 \times 10^{-19} \text{ C} = 4.80 \times 10^{-10} \text{ esu}$$

$$k = 1.38 \times 10^{-23} \text{ J/K} = 8.62 \times 10^{-11} \text{ MeV/K}$$

$$G = 6.67 \times 10^{-11} \text{ N m}^2 / \text{kg}^2$$

$$\alpha = e^2/(4\pi\epsilon_0\hbar c) \text{ (in SI)} = 1/137$$

$$m_e c^2 = 0.511 \text{ MeV}$$

$$m_p c^2 = 938 \text{ MeV}$$

$$(m_n - m_p)c^2 = 1.293 \text{ MeV}$$

$$1 \text{ u} = 931.49432 \text{ MeV}/c^2$$

$$1 \text{ pc} = 3.086 \times 10^{16} \text{ m} = 3.262 \text{ ly}$$

$$M_\odot = 1.99 \times 10^{30} \text{ kg}$$

$$L_\odot = 3.85 \times 10^{26} \text{ W}$$

1.3 Four forces of nature

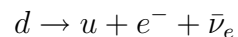
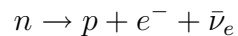
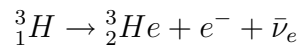
The *electromagnetic* (EM), *strong*, and *weak* forces have intrinsic strengths which are equal, or nearly so, at very short distances. The probed distance d is related to a characteristic momentum or energy (for example a collision energy) via the deBroglie relation $d = \lambda = h/p$. Since the ranges of the strong (~ 1 fm) and weak forces (< 0.1 fm) are finite, these forces become negligible for most purposes at distances greater than a few fm. For energies typical of the stellar cores, the weak force is typically much weaker than the strong force by something like a factor 10^6 .

A few tables which summarize basic properties of the four forces and elementary particles are provided from a separate link from the class web page.

The table below indicates which forces couple to the listed particles. All listed objects are subject to gravity, although it is utterly negligible at the atomic scale (or smaller) in stellar astrophysics.

object	EM	strong	weak
dogs, books, etc.	Y	N	N
electron, e	Y	N	Y
proton, p	Y	Y	Y
neutron, n	N	Y	Y
photon, γ	Y	N	N
neutrino, ν	N	N	Y
quark, u, d , etc.	Y	Y	Y

We need to look at some examples of the weak force, and to distinguish it from the strong force. A familiar example of weak interactions is β decay. Here is the same β -decay process, shown at increasing levels of sub-structure:

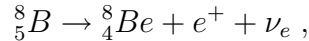


In the top line we have used the notation



for an atomic nucleus of element X , consisting of Z protons (atomic number) and $A - Z$ neutrons. The number A , known as the atomic mass, is the total number of nucleons (protons plus neutrons). The second line shows the same process at the *nucleon* level, that is at the scale of neutrons and protons. The third line gives the same process at the level of nucleon sub-structure, that is at the *quark* level. The quarks are, according to the Standard Model of particle physics, elementary particles, with no sub-structure.

We note that only the weak interaction can transform n to p or p to n . From the data in Section 1.2 we see that for a *free* neutron or proton, the process $n \rightarrow p + e^- + \bar{\nu}_e$ is energetically possible, but $p \rightarrow n + e^+ + \nu_e$ is not. How then can we understand the existence of the weak decay



which requires the $p \rightarrow n$ process? The point here is that the binding energies of the B and Be nuclei are different. In this case the 8_4Be nuclei is more tightly bound (larger binding energy E_b) than the 8_5B by an amount larger than the difference between p and n plus e^+ rest energies, making the process energetically possible. Figure 1 shows the binding energy per nucleon for all isotopes as a function of atomic mass A . We see that the maximally bound nuclei are in the vicinity of iron (Fe).

1.4 A process which gives hydrogen burning

We assume initially that the main sequence star under consideration consists entirely of hydrogen, or at least the presence of other elements can be ignored. As we have seen, a typical temperature in the core of a MS star like the sun is $T \approx 10^7$ K. The average kinetic energy of the constituents of a classical gas is

$$\bar{E} = \frac{3}{2}kT \approx 1 \text{ KeV} \tag{1}$$

for $T = 10^7$. Since this energy is much larger than the atomic binding energy of the hydrogen atom, the hydrogen is completely ionized. Hence the core is a dense gas of positively charged protons and negatively charged electrons.

We need to find a way for the protons to interact and *fuse* to form heavier elements. As Figure 1 shows, the creation of heavier elements (up to iron) will allow the binding energy of the product to be released as kinetic energy, thus providing the stellar energy source.

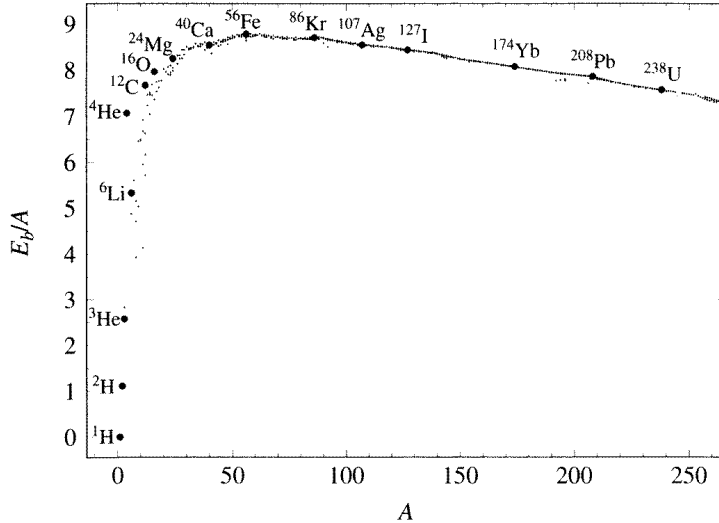


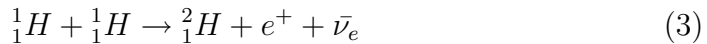
Figure 1: Binding energy per nucleon in MeV as a function of atomic mass A . (Figure 10.9 of Carroll and Ostlie.)

The most obvious potential candidate is $p + p \rightarrow {}^2_2\text{He}$. However, this state does not exist in nature — there is no proton-proton bound state.

We next consider the process which actually does take place, and is the first step for all stellar hydrogen burning:



or in nuclear notation:



where $d = {}^2_1\text{H}$ is the deuteron. We see that this process involves the (inverse) β decay process mentioned earlier: $p \rightarrow n + e^+ + \bar{\nu}_e$, where the resulting neutron forms the deuteron bound state with the surviving proton. So although the positive energy for this process results from the d binding energy due to the *strong* force interaction of n - p , this initial step utilizes the *weak* force. This is important, since, as we shall see below, the low rate for this weak process guarantees a long life for MS stars. Before we consider the reaction 3 and the remainder of the proton-burning sequence in more detail, we consider a simple model of the n - p bound state, the deuteron.

1.5 A simple model of the deuteron

An approximate form of the strong force for nucleons is the square well potential energy shown in Figure 2. The radius of the well of approximately $r_0 = 2$ fm and its depth of 36 MeV are based on the results of scattering experiments. When the Schrodinger equation is applied to this system with the n and p masses, one finds that only one bound state results with an energy eigenvalue of -2.2 MeV. This indeed corresponds to the experimental finding that the deuteron consists of only one bound state with a binding energy of 2.2 MeV.

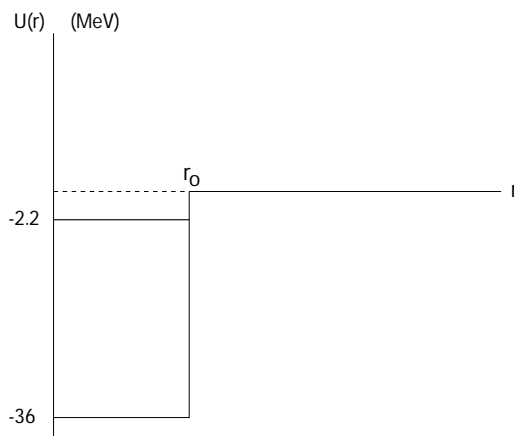


Figure 2: Square well model of the deuteron.

2 Stellar Energy Generation – PP-chain physics

2.1 The PPI chain and energetics

Figure 3 shows the main sequences by which hydrogen nuclei (protons) are converted into helium nuclei. The first step is the weak interaction process of Eq. 3. This step determines the rate of energy production in MS stars, and this property is the focus of the next two sections. Here, we look at the overall energetics of the processes.

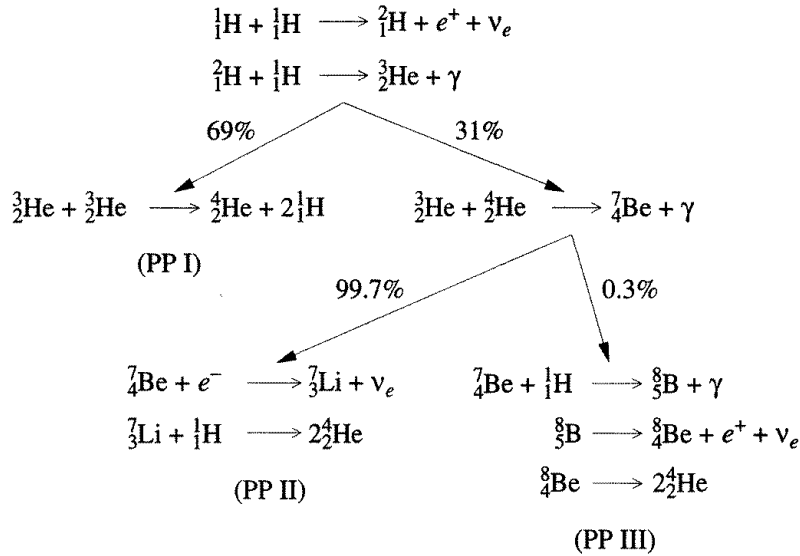
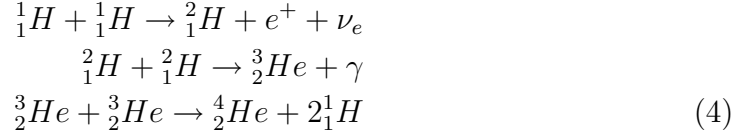


Figure 3: The PP chains. (Figure 10.8 of Carroll and Ostlie.)

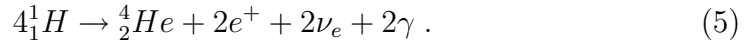
All three of the PP chains involve conversion of 4 protons to a helium-4 nucleus. Reference to 1 shows that ${}^4_2\text{He}$ is unusually stable relative to isotopes of similar atomic mass. In fact, ${}^4_2\text{He}$ is also known as an alpha particle, and due to its large binding energy and stability, is a typical by-product of nuclear reactions such as fission. Figure 3 shows a branching ratio of 69% for process 3 of the PPI chain. This reflects the probability of this path. However, the PPI chain accounts for 85% of the overall rate of ${}^4_2\text{He}$ production, and hence about 85% of the total energy output of the sun and similar MS stars. So we use the PPI chain to illustrate energy production, and in so doing we account

for the vast majority of the solar luminosity.

Rewriting the PPI chain:



We note that process 3 requires two reactions each of processes 1 and 2. So in sum there are 6 protons reactants and 2 proton products. Hence, the net effect of the PPI chain in terms of overall energetics is equivalent to:



We follow the usual practice in nuclear physics of using the *atomic mass unit*, or *u* for the rest masses of nuclei. By definition,

$$1u = \frac{1}{12}M({}^{12}_6\text{C}) ,$$

and a conversion to MeV can be made from Section 1.2. Using the AMU, the proton mass is 1.0078 u and the ${}^4_2\text{He}$ mass is 4.0026 u. So the energy available to the other final state particles, both as rest energy and kinetic energy, is

$$\Delta m = [4 \times 1.0078 - 4.0026] = 0.0287 \text{ u} ,$$

or $\Delta mc^2 = 0.0287 \times 931.49432 \text{ MeV/u} = 27 \text{ MeV}$. The positron rest mass will be available for kinetic energy, too, since it will annihilate with an ambient electron. So except for the energy given to the neutrinos, which exit the star without depositing any energy, the 27 MeV is available to provide the solar luminosity. (The neutrinos will be discussed separately in lecture 6.) We note that the first step of the PP chain, the *p-p* interaction, provides only about 0.3 MeV of kinetic energy.

So for each PPI reaction (*i.e.* for every 4 protons), the fraction of stellar mass which is converted to energy luminosity is (except for the neutrinos)

$$\epsilon = 0.0287/4.0313 \approx 7 \times 10^{-3} \tag{6}$$

Hence, the *available* hydrogen mass can be eventually converted into energy with an efficiency of 0.7%.

2.2 The pp interaction: Coulomb barrier penetration

The strong force for the n - p and p - p interactions are identical. (This is a symmetry property called *isospin*.) But we now have to add to this the Coulomb interaction between the protons:

$$U(r) = U_{\text{strong}} + U_{\text{coulomb}}, \quad U_{\text{coulomb}} = \frac{1}{4\pi\epsilon_0} \frac{e^2}{r} \quad (\text{SI})$$

This potential is depicted in Figure 4.

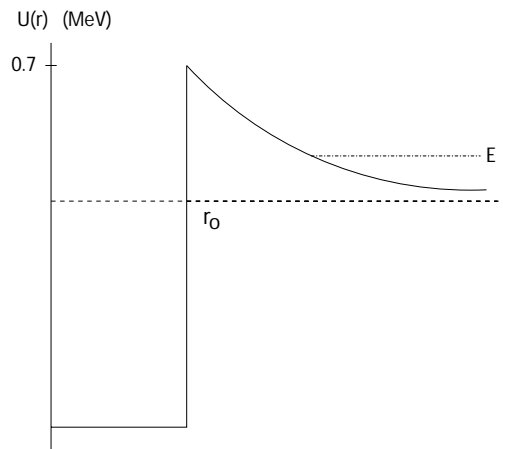


Figure 4: Potential energy model of the proton-proton interaction.

At $r = r_0 = 2$ fm we have (using SI units, then converting to eV):

$$U_{\text{coul}} = \left[(9 \times 10^9)(1.6 \times 10^{-19})^2 / (2 \times 10^{-15}) \right] \times 1 \text{ eV} / 1.6 \times 10^{-19} \text{ J} = 0.7 \text{ MeV}$$

So while the Coulomb barrier is 0.7 MeV, the average kinetic energy of the protons, from Equation 1 is ≈ 1 KeV. So classically, a proton at this average energy will never be able to get close enough to another proton to engage in strong or weak interactions. However, quantum mechanics provides the possibility of barrier penetration. We now sketch the solution to this calculation, which will be familiar to students who have had an introductory quantum course.

In the case of a 1-dimensional step potential of height U_b and width L , a particle of mass m and kinetic energy E has a barrier penetration probability P_G in the case where $E \ll U_b$ of $P_G \approx e^{-\gamma}$, where $\gamma^2 = 8mL(U_b - E)/\hbar^2$. For our potential of Fig. 4, where we assume spherical symmetry, we have an analogous solution to the 1-dimensional step potential, except that we now have to integrate over the Coulomb potential. So U_b is replaced by a geometrical factor multiplied by the barrier height. In the limit $E \ll 0.7$ MeV, which is our situation, the solution for the barrier penetration probability becomes

$$P_G dE \approx e^{-\gamma} dE, \quad \gamma^2 = E_G/E, \quad (7)$$

where E_G , known as the Gamow energy, depends on the composition of the charged-particle gas. In the present case for protons, this is

$$E_G = (2\mu_m/\hbar^2) \left[\frac{e^2}{4\epsilon_0} \right]^2 \quad (8)$$

in SI units, where μ_m is the classical reduced mass of the p - p system, $m_p/2$. The factor $1/4$ comes from the integral over the Coulomb barrier. Using combinations defined in Section 1.2 gives

$$E_G = \frac{1}{8} \frac{m_p c^2}{\hbar^2 c^2} (4\pi\hbar c\alpha)^2 = (938 \text{ MeV}) \left(\frac{\pi}{137} \right)^2 = 0.49 \text{ MeV}$$

Therefore, for an average proton kinetic energy of $\frac{3}{2}kT = 1$ KeV, we find the Coulomb barrier penetration probability to be

$$P_G \approx e^{-\sqrt{490/1}} \approx 10^{-10} \quad (9)$$

One can compare the probability above with that for which the protons exceed the classical Coulomb barrier because there is a small fraction which have thermal energies far above the average. For a classical, non-interacting gas the distribution of kinetic energies at a temperature T is given by the Maxwell-Boltzmann distribution:

$$P_{mb}(E)dE \propto E^{1/2} e^{-E/kT} dE \quad (10)$$

which follows the exponential decay form far above the average. For $kT \approx 1$ KeV, the probability of finding a proton at the Coulomb barrier is $\propto e^{-720}$

compared to the quantum barrier penetration factor which we found to be $\propto e^{-22}$. Clearly the thermal mechanism is insignificant compared to quantum tunneling in this case.

A correct determination of the probability of Coulomb barrier penetration should involve the convolution of the two distributions, of the form:

$$P_G(E) = \int_0^\infty P_q(E')P_{mb}(E - E')dE' \quad (11)$$

The resulting distribution, called the Gamow curve, has a maximum at about 5 KeV for a star like our sun.

2.3 Proton survival time

We can now estimate the rate of the initial hydrogen-burning process given in Equation 3. As stated earlier, this process is the slowest in the PP chain, and hence determines the rate of energy production in main-sequence stars. This rate is given by

$$R_{pp} = R_{\text{col}}P_G P_{pn} \quad (12)$$

where R_{col} is the pp collision rate, P_G is the barrier penetration probability of Equation 11, and P_{pn} is the probability that a barrier penetration results in the weak process $p \rightarrow n + e^+ + \nu$.

In class, we estimated the collision rate using the standard formulation $R_{\text{col}} = nv\sigma$, where n is the number density of protons, v is their average speed, and σ is the collision cross section. n is about 10^{26} cm^{-3} . We can find v from $\frac{3}{2}kT = \frac{1}{2}mv^2 = \bar{E} \approx 1 \text{ KeV}$, which gives $(v/c)^2 = 2\bar{E}/(mc^2) = 2/9.38 \times 10^5$, so $v \approx 4 \times 10^7 \text{ cm/s}$. And we find σ from the proton scattering radius ($\sim 1 \text{ fm}$), giving $\sigma \sim 10^{-26} \text{ cm}^2$. So then we have

$$R_{\text{col}} \approx (10^{26})(4 \times 10^7)(10^{-26}) \sim 4 \times 10^7 \text{ s}^{-1}$$

Because the weak force has such a short range, its strength is very small relative to the strong force for the rather large deBroglie wavelengths ($\lambda = h/p$) associated with the 1 KeV protons in the stellar cores. Therefore, even after a proton manages to penetrate the Coulomb barrier of the other proton, it is very unlikely that the weak process we need will occur rather than p - p elastic scattering via the strong interaction. Hence, we need to estimate

$$P_{pn} = P(p \rightarrow n + e^+ + \nu)/P(pp \rightarrow pp)$$

. We are now going to *revise and reformulate* the expression in Equation 12 compared to what was done in class in order to fill in the pieces more easily. We note that since the collision is dominated by strong p - p scattering at these energies, then $P_{pp} \approx P_{\text{col}}$. Furthermore, $P_{pn} = \Gamma_{pn}/\Gamma_{pp}$, where Γ is the transition rate (transition probability per unit time). Hence, we can re-write Eq. 12 as

$$R_{pp} = R_{\text{col}}P_G P_{pn} = N\Gamma_{pp}P_G(\Gamma_{pn}/\Gamma_{pp}) = NP_G\Gamma_{np} \quad (13)$$

where N is the number of protons available for the pp process. Now the rate for the weak β decay process can be used to evaluate Γ_{np} . It is a standard nuclear/particle calculation (see for example Halzen and Martin (1984)):

$$\Gamma = \frac{G^2}{\hbar\pi^3} \int_0^{E_0} p^2(E_0 - E)^2 dp, \quad (14)$$

where p and $E = \sqrt{p^2 + m_e^2}$ are the daughter electron's momentum and energy ($c \equiv 1$ momentarily), and E_0 is the binding energy difference between final and initial nuclei. (This calculation ignores many details, but should provide an order of magnitude estimate.) G is the Fermi (or weak) constant, which is related to the strength of the weak force: $G/(\hbar c)^3 = 1.2 \times 10^{-5} \text{ GeV}^{-2}$. An evaluation of the integral in the expression above is shown in Figure 5 as a function of E_0 . The relativistic approximation $p \gg m_e c$ often shown in texts is clearly not appropriate for binding energies of the p - p reaction. Using $E_0 = 0.3 \text{ MeV}$ for the p - p process, Eq. 14 yields $\Gamma \sim 10^{-7} \text{ s}^{-1}$. Combining this with the Coulomb barrier penetration probability Eq. 9, we find

$$R_{pp} \sim (N)(10^{-17}) \text{ s}^{-1}$$

Therefore, our order of magnitude calculation yields an average lifetime for protons in the core of solar-like MS stars of

$$\tau_p = N/R_{pp} \sim 10^{17} \text{ s}$$

or about 10 billion years, which is the appropriate time scale. Along with the overall energy output for the PPI chain found in the previous section, we now have a viable model for MS star energy generation.

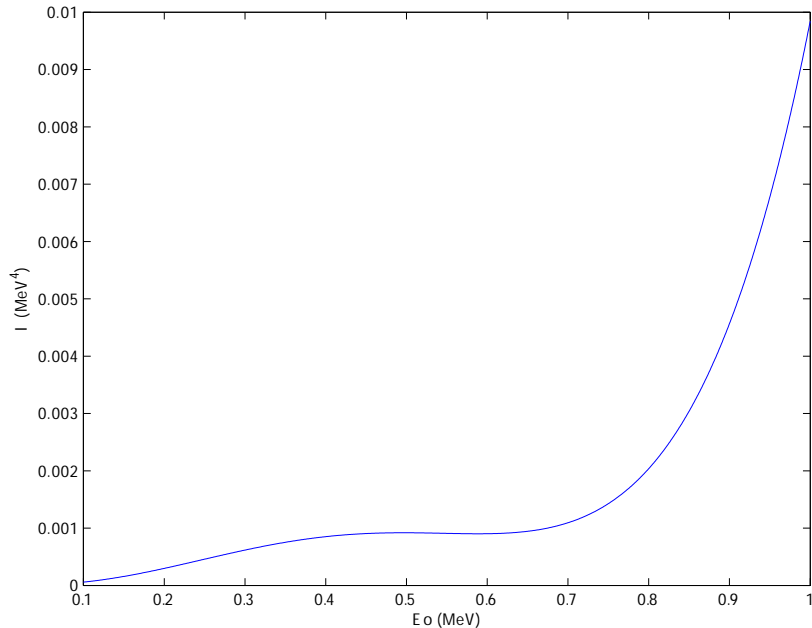


Figure 5: The integral in Eq 14 as a function of E_0 .

2.4 Other nuclear sequences

As discussed in Carroll and Ostlie, the temperature dependence of the PP chains is roughly given by $R_{pp} = \alpha_{pp}(T/10^6)^4$, where α depends on many other parameters. Other nuclear fusion processes are also possible. One example is the CNO cycle, depicted in Fig. 6.

Typically, these processes involve heavier nuclei, and the temperature dependence is much greater than the PP chain. For example, $R_{cno} = \alpha_{cno}(T/10^6)^{20}$. Two other chains, with even greater temperature dependence, are depicted in Figs. 7 and 8. The latter only becomes relevant for $T \sim 10^9$ K. The basic scenario for how these other chains come into play is as follows. For solar-like MS stars with a core temperature $\sim 10^7$ K. At this temperature, the PP rate dominates the rate, as expected. The higher- A processes have much lower rate at these temperatures, so represent a small correction to energy and element production. Now, since the equation of state gives a pressure $P \propto T$, in the steady state of hydrogen burning the PP will continue to dominate.

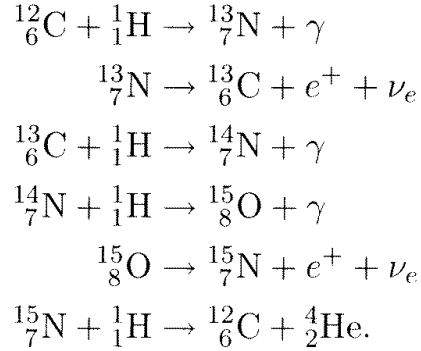


Figure 6: The main branch CNO chain. (Equation 10.51 of Carroll and Ostlie.)

However, as hydrogen is depleted the PP pressure is reduced, allowing further gravitational contraction, in turn requiring larger pressure to maintain mechanical equilibrium with a correspondingly larger T . The larger T rapidly increases the rate of the higher- A processes. So as the lighter nuclei are consumed, the burning of these elements will continue at layers at larger radius, while the inner core will involve the processes with heavier nuclei. These larger rates will consume the fuels relatively quickly. At some point in this evolution, electron degeneracy becomes important. This will be discussed in subsequent lectures.

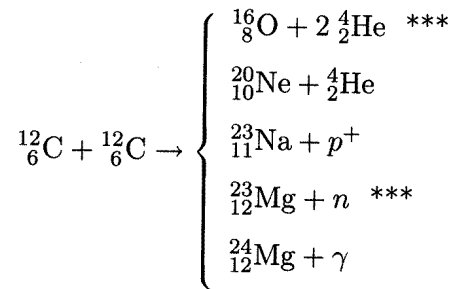


Figure 7: Another high-temperature fusion process. (Equation 10.59 of Carroll and Ostlie.)

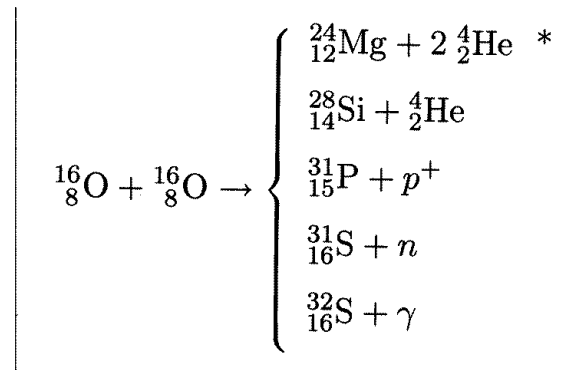


Figure 8: Yet another high-temperature fusion process. (Equation 10.60 of Carroll and Ostlie.)

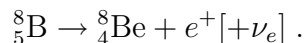
3 Solar neutrino physics

Nuclear processes in stellar cores produce large numbers of neutrinos of energy ~ 1 MeV. The feeble interaction of neutrinos with matter ensures that they exit the core and star with near 100% transmission. This makes neutrinos a unique probe of stellar astrophysics. Here we focus on MS stars, specifically the sun. The underlying physics, the story of solar neutrino detection, and the “solar neutrino problem,” and its resolution are briefly discussed in this lecture.

3.1 Neutrinos are elementary particles

We discussed neutrinos earlier in our brief introduction to the elementary particles. Because the neutrinos couple only to the weak force, they are very difficult to detect directly. It is not so much that the weak force has a small intrinsic strength — the coupling constant is actually slightly larger than the electromagnetic coupling. The weak force, however, has a very short range. So while at an energy ~ 100 GeV, the strength is comparable to EM, at low energy, where the deBroglie wavelength is large compared to the force range, the effective strength is tiny. The range helps us understand why the primary neutrino cross sections obey $\sigma \propto E^2$ for $E \ll 100$ GeV, which is the range of interest for us.

A neutrino interaction was not directly observed until 1956 by Reines and Cowan. However, their existence was inferred and expected beforehand. In 1932 Pauli predicted their existence. He based this on the observed energy spectra of electrons or positrons from beta decay processes such as



If the final state really consisted only of 2 bodies, then E_e is a constant, depending only on the masses involved. Instead, a continuous distribution was observed for E_e . Pauli reasoned that either energy is not conserved in such decays (!) or an undetected particle was present in the final state. . . the neutrino.

There are 3 species of neutrinos, ν_e , ν_μ and ν_τ , one in each of the 3 “generations” of elementary particles. However, with notable exceptions, most processes we consider in astrophysics involve only generation 1 (this is the lightest), so we mostly encounter ν_e (and $\bar{\nu}_e$). Neutrinos were originally assumed to be massless. However we now know their masses to be finite, in

part due to the solar neutrinos discussed below. Their mass values are not known, but they are small, likely to have $m_\nu \ll 1 \text{ eV}/c^2$.

3.2 Predictions for neutrino production

A simple calculation provides a good estimate of the expected flux of solar neutrinos at the earth. By first approximation, the PPI chain provides the solar power we observe on earth. As discussed in lectures 4 and 5, every iteration of this sequence results in $2 \nu_e$ and 27 MeV of kinetic energy, which we observe eventually as luminosity. This luminosity corresponds to a power of $137 \text{ mW}/\text{cm}^2 = 8.53 \times 10^{11} \text{ MeV}/(\text{cm}^2 \text{ s})$. Hence, we expect the neutrino flux at earth to be

$$8.53 \times 10^{11}/(27/2) = 6.4 \times 10^{10} \nu_e'/\text{s}/(\text{cm}^2 \text{ s}).$$

Figure 9 is the state of the art prediction of the overall solar neutrino flux at earth from Bahcall, *et al.* The estimate above is indeed rather close to the calculated PP flux. The peaking of the curves near the maximum energy is due to the parity-violating nature of the weak interaction. We note that although the PP neutrinos dominate the flux, their energy is limited to below $\approx 0.4 \text{ MeV}$. The neutrinos from 8_5B decay on the other hand extend to about 15 MeV.

3.3 Solar neutrino detection

Detection of neutrinos in general is difficult. In high-energy (*i.e.* elementary particle) physics, neutrino beams can be produced and used as a very incisive probe of the weak force. However, this is only practical because the interaction probability (cross section) increases rapidly with energy, as noted earlier. Hence, for a neutrino in a beam with energy $\sim 100 \text{ GeV}$, the interaction rate is large enough so that an experiment at Fermilab called NuTeV was able to collect a few million neutrino events over about a year of data collection. (These were the pictures I showed in class of a huge “splat” of energy in the center of large quantity of iron.) The experimentalist hoping to measure solar neutrinos does not have the advantage of such high energy, although the flux of neutrinos is large, as seen above.

Figure 10 summarizes the principal detectors used to measure solar neutrinos over the last few decades. The field was pioneered by R. Davis, who

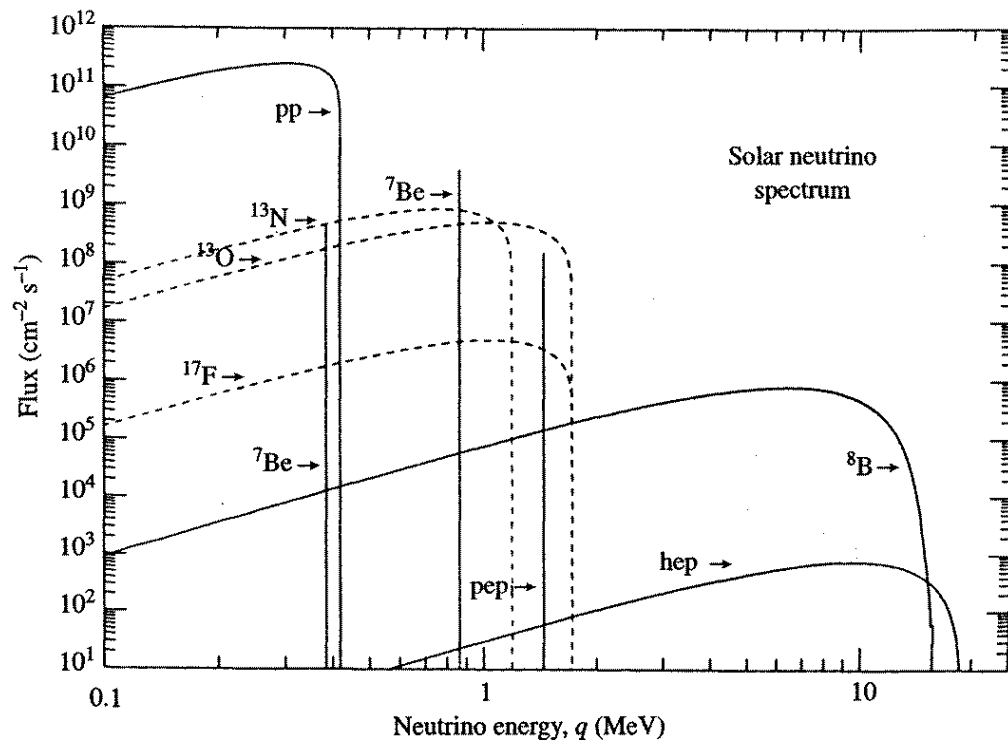
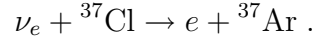


Figure 9: Predicted solar neutrino spectra – the flux at earth as a function of neutrino energy. (From Bahcall.)

came up with a viable detector consisting of a large vat of cleaning fluid deep underground (in a mine at Homestake, SD). The experiment is sensitive to neutrinos in the reaction



The resulting argon gas bubbles out and is extracted. Since this isotope of argon is unstable, its quantity is determined by measuring the decay curve. All solar neutrino experiments are deep underground, so that cosmic ray particles are filtered out by the overburden. The Davis experiment ran for about two decades with a measured flux which on average was $(34 \pm 3)\%$ of the predicted flux before the result was confirmed by other experiments. In the meantime, there was a great deal of debate about the result. Davis's experiment was primarily sensitive to 8B neutrinos, since its threshold is above the PP neutrinos. Could the solar theory be trusted for non-PP sequences, where there are such large temperature dependences (see lecture 5)? The discrepancy between theory and experiment was known as the *solar neutrino problem*.

Experiment	Reaction	Threshold (MeV)	Observed/expected rate
SAGE + GNO	CC ${}^{71}\text{Ga}(\nu_e, e){}^{71}\text{Ge}$	0.2	0.58 ± 0.04
HOMESTAKE	CC ${}^{37}\text{Cl}(\nu_e, e){}^{37}\text{Ar}$	0.8	0.34 ± 0.03
SNO	CC $\nu_e + {}^2\text{H} \rightarrow \text{p} + \text{p} + \text{e}$	~ 5	0.35 ± 0.03
SUPER-K	ES $\nu + \text{e} \rightarrow \nu + \text{e}$	~ 5	0.46 ± 0.01
SNO	ES $\nu + \text{e} \rightarrow \nu + \text{e}$	~ 5	0.47 ± 0.05
SNO	NC $\nu + {}^2\text{H} \rightarrow \text{p} + \text{n} + \nu$	~ 5	1.01 ± 0.12

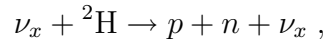
CC = charged current (W exchange); NC = neutral current (Z exchange); ES = electron scattering (via NC for ν_μ, ν_τ , and via NC and CC for ν_e).

Figure 10: Main solar neutrino detectors and measured fluxes. (From Perkins.)

The next big breakthrough was the gallium experiments, SAGE and GNO. The technique was similar to the Davis experiment, except using gallium as the target, which has a threshold of only 0.2 MeV in the process indicated in Fig. 10. These experiments were sensitive to the PP neutrinos, and their detected flux was roughly half that expected by theory. Meanwhile,

the Super-K experiment in Japan had also confirmed the missing high-energy flux using a technique which allowed them to actually image the direction of the neutrinos, confirming their solar origin. The detectors using water as a neutrino target rely on the following principle. The solar neutrinos collide with an atomic electron, sending it out into the water as a free particle with a speed close to c . This is faster than the speed of light in the water, which has speed c/n , where n is the index of refraction. This results in a shock-wave phenomenon known as Cherenkov radiation, which can be detected by sensitive light detectors (photo-multiplier tubes) installed on the periphery of the water tank.

The “problem” was finally resolved a few years ago by the SNO experiment. Recall that we know that there are 3 species of neutrino, ν_e , ν_μ , and ν_τ . The Davis and gallium experiments could only measure the ν_e type. Since only ν_e are produced in the nuclear reactions in the sun, this may not seem to be an issue. However, we note that the Super-K measurements were slightly sensitive to the other two types, and they measured a higher rate. The SNO breakthrough was that its detection target material is *heavy water*, that is H_2O where the H is largely deuterium, 2_1H . As we said in lecture 4, the deuteron is very weakly bound. Hence a neutrino of a few MeV energy can disassociate the deuteron. The resulting charged proton can be observed by the Cherenkov technique. This process,



is equally likely for any of the 3 neutrino species, x .

The SNO result for this reaction is consistent with the predicted solar flux. This means that the “problem” was not a problem with the solar theory, but rather indicated a new property of the neutrinos themselves, as discussed briefly below. The ν_e type produced in the solar core were turning into the other species with some probability on their journey to the earth. The other detectors only saw the remaining ν_e 's, but SNO saw them all. Hence, SNO not only confirmed the origin of the “problem,” but also confirmed that the solar theory indeed predicted the correct neutrino flux. Davis shared the 2002 Nobel Prize in physics.

3.4 Neutrino oscillations and mass

To illustrate the point, we discuss only two neutrino species. The generalization to three is qualitatively the same, but is more complicated. Let the

neutrino species have small, but finite masses, with values (eigenstates) m_1 and m_2 . The quantum state for m_1 will in general be a linear combination of ν_e and ν_μ . The state begins as ν_e , as determined by the weak interaction process in the solar core. Now, quantum mechanics requires that the mixed state evolve in time according to

$$\psi(t) = \psi(0)e^{-i(\Delta E)t/\hbar} ,$$

where ΔE is the energy difference of the states. Relating this to the mass eigenstates and t to the distance travelled, the probability for transition from one type of neutrino to the other, called *neutrino oscillation*, over a distance L (in km) in vacuum becomes:

$$P_{1\rightarrow 2} = P_{2\rightarrow 1} = \sin^2(2\theta) \sin^2 \left(1.27 \Delta m^2 L/E \right) \quad (15)$$

at an energy E (in GeV), and $\Delta m^2 = m_2^2 - m_1^2$ is in eV^2/c^2 . The parameter θ determines the linear combination $\psi_1 = \cos\theta \psi_e + \sin\theta \psi_\mu$ and is called the mixing parameter. One additional detail: While the neutrinos do not get significantly absorbed by the sun on their outward trek, there is an interesting resonance effect where the neutrino mass difference matches the ambient mass density. The interaction is analogous to light passing through transparent material with index of refraction > 1 . The effect is called MSW enhanced oscillations, and can easily result in maximal mixing of the neutrino states, *i.e.* $\tan\theta \approx 1$. In this case we would also expect the ratio of ν_e to total flux at earth to be $\approx \frac{1}{2}$, with some energy dependence from Equation 15. The data are consistent with both of these predictions.

Hence, the resolution of the solar neutrino problem requires finite neutrino masses. This effect has also been seen in other types of neutrino experiments, so it is known that all 3 types mix with each other. While only Δm^2 is directly measured, the implications from all the data are quite strong that the individual masses are very small, $m \ll 1 \text{ eV}/c^2$. If this is indeed the case, as we shall see later, this makes neutrino mass irrelevant for cosmology.

4 Type II Supernova Physics

We consider the physics and phenomenology of supernovae, energetic explosions of stars, focussing on the so-called Type II type of supernova, which involves an evolved, massive star which is not necessarily a member of a binary system. As discussed in the next lecture, a supernova event produces a shock wave of rapidly expelled stellar material which is bombarded by a huge neutron flux. Neutron capture events result, leading to the production of elements heavier than iron and nickel, which we haven't been able to produce in the stellar processes discussed so far. Hence, heavy elements are produced exclusively by supernovae, and the development of earth and its life forms depend on at least one cycle of heavy star evolution and subsequent supernovae.

4.1 Massive star core collapse sequence

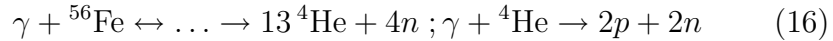
Consider an “evolved” star, one which has evolved off the main sequence and has an evolved mass M which may be significantly smaller than its zero-age main-sequence (ZAMS) mass. As discussed in previous lectures, at some point the pressure due to electron degeneracy becomes important. This is the pressure which results from electrons being forced to higher-energy states due to the Pauli exclusion principle, which applies to all fermions (spin= $\frac{1}{2}\hbar$ particles), such as electrons or neutrons. Now if $M < 1.4M_{\odot}$, then the electron gas is non-relativistic, and the electron pressure is $\propto n^{5/3}$, where n is the electron number density, and the star is stable under gravitational collapse, since the gravitational pressure is $\propto n^{4/3}$. The fate of such a star is a white dwarf, as discussed before. The mass $1.4M_{\odot}$ is known as the Chandrasekhar mass.

However, if the evolved mass is $> 1.4M_{\odot}$, then the electron gas is relativistic, the electron pressure is $\propto n^{4/3}$, and the star is in unstable equilibrium with the gravitational pressure. Eventually, an unstable equilibrium always moves toward a stable equilibrium at with lower potential energy configuration. A massive, evolved star would eventually have a core temperature of $\sim 5 \times 10^9$ K and a density of $\sim 3 \times 10^{10}$ kg/m³. The average thermal kinetic energy of nucleons is then ~ 1 MeV and the Boltzmann distribution extends to sufficiently high energy to allow fusion of nuclei up to nickel and iron (see Figure 1 from Lecture 4). After iron, it is energetically unfavorable to go to higher atomic number, so the massive star develops an iron core with silicon

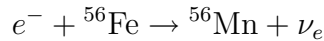
burning in the next sub-shell outward in radius. The silicon eventually ends up as iron, too, but after about one day this fuel is exhausted. Our massive star is now in unstable mechanical equilibrium, supported only by the electron degeneracy pressure.

The following describes what is thought to be a typical sequence of events for the collapse of a massive star, resulting in a *supernova* event. However, keep in mind that rotation and magnetic fields, which we have ignored so far, may have an important role, although the outcome is unlikely to change significantly.

1. After fusion processes fizzle out, there is some gravitational collapse which causes heating to $T \sim 10^{10}$ K. This is sufficient to trigger two processes:
 - (i) Photo-disintegration of iron and the subsequent photo-disintegration of the products, eventually leading to complete “inverse fusion,” with products p and n :



- (ii) Inverse beta decay. When electrons have $K > 3.7$ MeV then the following can occur:



and by time we get down to nucleons:



Note that the Fermi energy of the degenerate electron gas is ≈ 4 MeV at a density of 10^{12} kg/m³, so there are plenty of electrons which can trigger these inverse beta decays.

2. The processes above are *endothermic*, that is they remove kinetic energy (and hence fluid pressure) from the core. The unstable core now quickly collapses.
3. The iron core is now in free fall. The time of fall to a much smaller equilibrium radius is ~ 100 ms.

4. During collapse, the *neutronization* processes in Eqs. 16 and 17 proceed rapidly. Neutrinos result as well, and these mostly exit the star. This neutrino emission represents about 1% to 10% of the total emission, the remainder resulting from subsequent steps.
5. The collapse ends when the core reaches nuclear density. Actually, the density exceeds nuclear briefly by what is estimated to be a factor of 2 to 3. This is discussed with some more detail in Section 4.3 below.
6. The core now strongly *bounces* back to nuclear density from the super-nuclear density. We can think of the protons and neutrons as bags of quarks bound together by very strong springs (spring constant ~ 10 GeV/fm²) which are compressed by the collapse, but then spring back to equilibrium, thus the bounce.
7. The bounce sends a shock wave outward at high velocity, blowing off the remaining stellar atmosphere in the process. One the shock reaches the outer atmosphere, the photons emitted by recombination, powered by the shock itself and by subsequent nuclear decays, become the visible supernova explosion.
8. The core will radiate away its huge energy content in neutrinos, as discussed below, and the remnant core will settle down into a *neutron star*. The radius is something like 15 km, depending on initial core mass, but has a mass of 1.4 to about $3 M_{\odot}$.
9. The neutron-rich shock, meanwhile, will induce creation of elements heavier than iron by neutron capture. This will be discussed in the next lecture in more detail.
10. The shock continues into interstellar space at speeds of $\sim c/10$. For example, the crab neubula, resulting from the 1054 A.D. supernova is large and still expanding.
11. The neutron star may become visible in radio as a *pulsar*, depending on rotation and magnetic fields. The crab's neutron star is indeed a very "loud" pulsar, faithfully producing a radio burst once per revolution, every 33.3 ms.

The visible-light luminosity of a typical supernova is roughly 10^{42} J, with a peak power of 10^{36} J/s = 10^{36} W. This is about a factor 10^{10} greater than the

solar luminosity, which is comparable to an entire galaxy. The visible light decays exponentially as unstable nuclei decay, so the supernova is visible for weeks, depending on its location. This is discussed more in the next lecture. However, as impressive as the light output is, it represents only about 1% of the total energy output, as we shall see in Section 4.4. We follow up now with some detail.

4.2 Energy from collapse

We saw earlier that the total gravitational energy released in collapse is the change in potential energy given by

$$E_{\text{grav}} = \frac{3}{5} \frac{GM^2}{R}$$

when the final radius R is much smaller than the initial. (In our case, the ratio is $\sim 10^{-3}$.) Using $M = 1.5M_{\odot}$, that is, just over the Chandrasekhar limit, then with $R = 15$ km we get

$$E_{\text{grav}} = 6 \times 10^{46} \text{ J} = 4 \times 10^{59} \text{ MeV} \quad (18)$$

This is a big number! It will feed into the energy release of the supernova.

4.3 A very large nucleus

As mentioned above, the collapse proceeds to nuclear density, where it is halted by the strong nuclear force. It takes collision energies of ~ 10 GeV to partially break up a nucleon (neutron or proton). As we shall see momentarily, the average energy from the collapse is still 2 orders of magnitude from this. So the nucleons, predominantly neutrons at this point, get squeezed by the collapse to sub-nuclear volume, then rebound, giving rise to the supernova bounce and the return to nuclear density.

So we are justified in treating the collapsed core as closely packed nucleons, essentially at nuclear density, and consisting primarily of neutrons. As we saw with the electrons, the neutrons will also form a degenerate “gas” since they are fermions. We return to this briefly at the end. In any case, the collapsed core will settle down into what is termed a *neutron star*.

Nuclear density ρ_N we can estimate by the average density of a proton (or neutron):

$$\rho_N = m_p / (4\pi r_o^3 / 3) = 2 \times 10^{17} \text{ kg/m}^3 ,$$

where we have used $r_o = 1.2$ fm for the proton radius, based on lab scattering measurements. With ρ_N as the average nuclear density, then the total mass of this proto-neutron star is

$$M_{ns} = Nm_p = \rho_N 4\pi R^3/3 ,$$

where N is the total number of nucleons (neutrons). Combining these, and using $M_{ns} = 1.5M_\odot$ yields:

$$R = r_o N^{1/3} = 15 \text{ km} ; \quad N = 1.5M_\odot/m_p = 2 \times 10^{57} . \quad (19)$$

Combining Eqs. 19 and 18 gives an estimate for the average energy per nucleon of $(3 \times 10^{59}/(2 \times 10^{57})) \approx 100$ MeV/nucleon. This number provides two lessons:

- It is a large kinetic energy, but far short of what is required to break up the nucleons.
- Recall from Fig. 1 of Lecture 4 that iron had the largest binding energy per nucleon at 8 MeV/nucleon. The collapse provides more than enough energy to completely break up even iron into constituent nucleons, as we had presupposed.

4.4 The first seconds of the proto-neutron star

Because the proto-neutron star is so dense, a qualitatively new feature is manifest. Namely, the vast majority of the collapse energy of Eq. 18 can not easily escape. To see this, we calculate the mean free path of the most weakly interacting particles, the neutrinos.

As we saw in Lectures 5 and 6, the collision rate is given by $n\sigma v$, where n is the number density and σ is the interaction cross section. Hence, the time between collisions is the inverse of this; and the mean distance between collisions (the *mean free path*) is $\ell = v/(n\sigma v) = 1/(\sigma n)$. In this case, $n = N/(4\pi R^3/3)$ and σ is the neutrino-nucleon cross section. The so-called charged-current cross section for the process $n + \nu_e \rightarrow p + e^-$ is given by

$$\sigma_{cc} = \frac{5.8}{\pi} G_F^2 E^2 \approx 10^{-45} \left(\frac{E}{1 \text{ MeV}} \right)^2 \text{ m}^2 ,$$

where G_F is the weak (Fermi) coupling constant encountered in Lecture 5. If we use $E_\nu = 20$ MeV, this gives $\ell \approx 2$ m ! The mean free path for neutrinos attempting to escape the collapsed core is only a few meters.

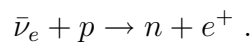
As it turns out, the neutral current scattering process $\nu_x + n \rightarrow \nu_x + n$ is also possible here, where x represents any of the 3 neutrino species. A similar calculation (a bit more complicated) for this process gives $\ell \approx 10$ m. Hence we arrive at the following conclusions:

- The collapse energy is locked in the proto-neutron star and can only be carried away by neutrinos. Estimates are that about 99% of the total energy of collapse is carried by the neutrinos.
- The neutrinos are radiated from a thin few meter thick skin on the outside of the core.
- With $\ell \sim 10$ m, the energy transport via neutrinos is a random walk, diffusion problem. We can estimate the diffusion time to be $t \sim R^2/(c\ell) \sim 1$ s. This compares to a speed of light flight time of $\sim R/c \sim 10^{-4}$ s.
- There are effectively 6 neutrino populations in thermal equilibrium with the super-hot core – 3 species, with both neutrinos and anti-neutrinos. These all share the energy transport via the neutral current process. Hence we expect the 150 MeV/nucleon to be carried away with an average energy per neutrino of $150/6 \approx 20$ MeV.

Thus, along with the visible supernova, we expect a huge neutrino flux equal to the collapse energy $\sim 10^{59}$ MeV carried by about 10^{58} neutrinos in all 3 species and ν plus $\bar{\nu}$ with average energy 20 MeV.

4.5 SN1987a

In 1987 supernova was observed at earth located in the large magellenic cloud (LMC), a small galaxy adjacent to the milky way, at a distance of about 60 kpc. Luckily, two underground proton decay experiments were taking data. These detectors can observe neutrino events using the water technique discussed in Lecture 7a. (In fact, one of the detectors, Kamiokande, later became the Super-K detector encountered in 7a.) The two detectors simultaneously observed a burst of neutrino events about 7 hours before the optical supernova was observable. The predominant detection process was



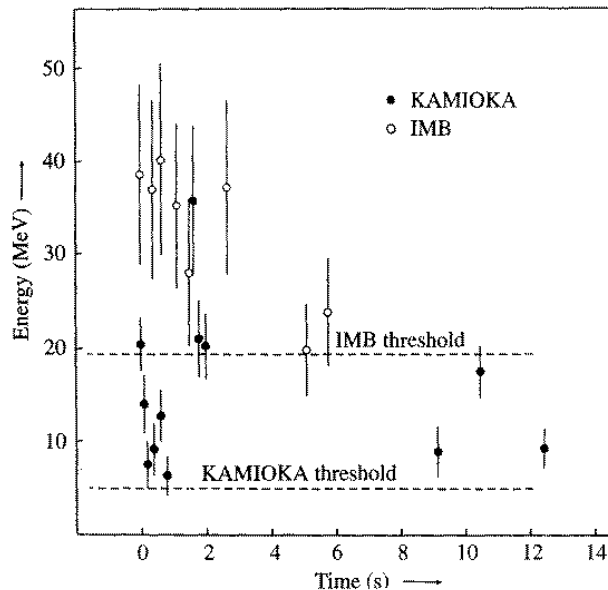


Figure 11: Neutrinos detected from SN1987a with the IMB and Kamiokande detectors.

The neutrino data is reproduced in Fig. 11.

We can now compare the observations with our expectations. The measured neutrino energy is indeed about 20 MeV. (The apparent decline with time can be used to determine neutrino mass. The limit turns out to not be better than terrestrial experiments.) The neutrinos are indeed spread out in time by ~ 1 s. (Again, finite neutrino mass can disperse this somewhat.) The number of detected events was 20. Only $\bar{\nu}_e$ were observed, so the total flux at earth was $20 \times 6/\sigma_d \approx 10^{10}/\text{cm}^2$, where σ_d is the detection cross section times efficiency. Translating this flux to the distance of the LMC gives a total energy of 2×10^{59} MeV, in good agreement with our expectations from the previous section.

It is interesting to note that the neutrino burst from the collapse may in fact transfer enough energy to the supernova shock front to keep it from falling back onto the collapsed core. This may, in fact, require all 3 neutrino species (although the calculations are difficult), in which case we would require the 3 species to make heavy elements (and life on earth).

4.6 Further collapse and black holes

We discussed collapse stoppage and bounce above in terms of the strong nuclear force. However, since we form a core of mostly neutrons, we might expect neutron degeneracy to also play a role. And it does. As the proto-neutron star radiates away its collapse energy we might expect it to undergo further collapse if not for the degeneracy pressure. Carrying out the same calculation we did earlier for electrons results in an equivalent Chandrasekhar mass of about $5.6M_{\odot}$. If the collapsing core mass exceeds this, then we might expect the collapse to proceed to a black hole. If less, then it remains a neutron star.

However, the observed transition from neutron star to black hole is closer to $3M_{\odot}$. We might have expected that this would not be so simple. Among the complicating factors, all difficult to calculate, but important in this regime, are:

- repulsion due to the strong nuclear force
- neutron degeneracy
- non-linear gravity; that is, strong gravitational effects, as predicted by General Relativity
- large angular velocity
- large magnetic fields

On the note of strong gravity, we finish by mentioning the Schwarzschild radius, R_s , predicted by GR as the “event horizon” where proper time intervals go to zero and light cannot escape. It is given by

$$R_s = 2GM/c^2 .$$

For $M = 5M_{\odot}$, $R_s \approx 15$ km, comparable to the size of our neutron star, but with larger mass. Adding mass to a neutron star would result in a black hole. If the initial collapsing core had mass $\sim 5M_{\odot}$ or more, the collapse might proceed directly to a black hole, although many researchers believe there would be a stopping bounce followed by infall back onto the collapsed core, leading then to a black hole.

5 Cosmological expansion

In this lecture we discuss Hubble’s observation of galactic redshifts in the context of general relativity. The *cosmological principle* provides simplifying assumptions, allowing to an “equation of motion” for the scale factor R known as the Friedmann equation. This equation will be a starting point for many of our discussion of physics of the early universe.

5.1 Spacetime in Relativity

In special relativity, a key concept is the invariant spacetime interval ds^2 :

$$ds^2 = (c dt)^2 - (dx^2 + dy^2 + dz^2) ,$$

which separates two points in spacetime. The interval ds is the same for any observer in an inertial reference frame. It can also be written equivalently as

$$ds^2 = \sum g_{\mu\nu} dx_\mu dx_\nu ,$$

where $g_{\mu\nu}$ is the metric tensor and $dx_\mu = (ct, x, y, z)$ are 4-vectors. For the flat spacetime of special relativity, $g_{\mu\nu}$ is the Minkowski metric, represented by a 3×3 matrix with diagonal elements 1, -1 , -1 , -1 , and all other elements zero.

In spherical coordinates, then the interval in flat spacetime becomes:

$$ds^2 = (c dt)^2 - dr^2 - r^2 (d\theta^2 + \sin^2 \theta d\phi^2) .$$

This can be compared with the Schwarzschild interval which is a solution of the equations of general relativity for the case of spherical symmetry at a distance r from a mass M :

$$ds^2 = \left[1 - \frac{2GM}{rc^2} \right] (c dt)^2 - \left[1 - \frac{2GM}{rc^2} \right]^{-1} - r^2 (d\theta^2 + \sin^2 \theta d\phi^2) . \quad (20)$$

The proper time $d\tau$ measured by a clock at rest at a distance r from the mass is given by

$$(c d\tau)^2 = \left[1 - \frac{2GM}{rc^2} \right] (c dt)^2 ,$$

where dt is the time measured in a distant inertial frame. We see that as one approaches the distance $r = 2GM/c^2 \equiv R_s$, the proper time interval

approaches zero. This distance R_s is the Schwarzschild radius encountered before, representing the horizon of a black hole.

Finally, under the assumptions that the universe is isotropic and homogeneous, the FLRW interval result for general relativity is

$$ds^2 = (c dt)^2 - R(t)^2 \left[\frac{dr^2}{1 - Kr^2} + r^2 d\theta^2 + r^2 \sin^2 \theta d\phi^2 \right], \quad (21)$$

where $R(t)$ is the *scale parameter* and K represents the type of spacetime curvature. The equations can be re-scaled so that K conventionally can take on one of three discrete values:

- $K = 0$. Flat spacetime. The 2-d analog is a flat sheet.
- $K = +1$. Positive curvature. The surface of a balloon in 2-d.
- $K = -1$. Negative curvature. A saddle point in 2-d.

The scale parameter $R(t)$ represents the fractional expansion of the distance between two points due to cosmological expansion (see next sections). So if r_o is a distance between two objects, then at a later time, the true coordinate distance between the objects has become $r(t) = R(t) r_o$. (r_o is known as the comoving coordinate distance.) Note that $R(t)$ is only a function of time.

5.2 Hubble's Observation and its interpretation

The redshift z measures the fractional shift of the observed wavelength λ' of a spectral feature, *e.g.* an emission line, relative to the wavelength λ of the feature measured in a proper frame. So $z = \Delta\lambda/\lambda = (\lambda' - \lambda)/\lambda$, or

$$\lambda' = \lambda(1 + z) \quad (22)$$

Hubble observed redshifts for tens of relatively nearby galaxies for which their distance was independently known. The relativistic Doppler shift provides an explanation for a shift of wavelength due to the motion v of the source with respect to the observer:

$$\lambda'/\lambda = \left[\frac{1 + (v/c)}{1 - (v/c)} \right]^{1/2} \approx 1 + \frac{v}{c},$$

where the approximation is valid only for $v \ll c$. Combining this with Eq. 22 gives $z \approx v/c$, which Hubble used to then arrive at his hypothesis:

$$v = H_o r .$$

H is the Hubble parameter, and the subscript refers to its value at our current epoch. The presently accepted value of H_o is about 70 (km/s)/Mpc.

The interpretation of the galactic redshifts in terms of a Doppler shift fails to be consistent with the data at larger values of z . In addition, it implies that the Earth (or at least our galaxy) is in a unique position in the universe. It violates the *cosmological principle*, that the universe, at sufficiently large distance scales, is isotropic and homogeneous. Consistency with this principle implies that spacetime itself is expanding, along with its contents, and that the expansion was initiated a singular event, the big bang. As we will see, this hypothesis is consistent with all well-defined predictions to date, including the redshifts, and has successfully predicted a large number of diverse observations.

It is natural to describe the cosmological expansion using general relativity. The scale parameter R introduced above, now becomes the key quantity used to describe the expansion of spacetime. Two important relations follow immediately. The scale parameter at a time t after the big bang corresponding to an observed distant object at redshift z is related to the current scale R_o by

$$R(t) = R_o / (1 + z) . \tag{23}$$

And Hubble's hypothesis can be re-written as

$$\dot{R} = H R , \tag{24}$$

where we have introduced the notation $\dot{f} = df/dt$. We note that if H were a constant (is is *not*), then Eq. 24 becomes $dr/R = H dt$, which is integrated to give $R(t) \propto e^{Ht}$. In this case, the size of the universe increases by a factor e in a time

$$t = 1/H_o = 14 \text{ Gyr} . \tag{25}$$

This time $1/H_o$ is known as the *Hubble time*.

Finally, we note that the cosmological principle *does not* mean that the universe can not have dramatic structure – in fact, it does – only that such structure averages out over sufficiently large (*i.e.* cosmological) distance scales to look the same in all directions and at all locations.

5.3 The Friedmann equation and a useful analog

The field equations of general relativity can be written in tensor form

$$G_{\mu\nu} = 8\pi GT_{\mu\nu} + \Lambda g_{\mu\nu} , \quad (26)$$

where $T_{\mu\nu}$ is the stress energy tensor, which contains the description of the mass and energy densities, $G_{\mu\nu}$ is the Einstein tensor, which gives the resulting spacetime curvature, and Λ is the (infamous) cosmological constant. We will not use this equation directly, in which many ordinary equations are embedded.

Invoking the cosmological principle, and assuming matter and radiation fields can be described as ideal frictionless fluids (more on this part later), Friedmann found the following solution to Eq. 26 in terms of the scale parameter R :

$$H^2 = \left(\frac{\dot{R}}{R}\right)^2 = \left(\frac{8\pi G}{3}\right) \rho_{\text{tot}} - \frac{Kc^2}{R^2} \quad (27)$$

Here, ρ_{tot} is the total energy density and K is the curvature parameter introduced above.

We can gain significant intuition about the Friedmann equation by showing its equivalence to a more familiar model. Let us assume that ρ is dominated by ordinary non-relativistic matter and that this density is uniform. We put a test mass m at the edge of a sphere of radius $R(t)$. Only the mass within the sphere, $M = 4\pi R^3 \rho/3$, contributes to the gravitational force acting on m . (This Gauss's Law for gravity also holds in general relativity.) Hence, the potential energy of m is $-GMm/R$, and the total energy $E = E_K + U$ is

$$\frac{1}{2}m\dot{R}^2 - \frac{GMm}{R} = E .$$

Substituting $M = 4\pi R^3 \rho/3$ and multiplying through by $2/(mR^2)$, then the left-hand side is identical to Eq. 27. And the right-hand side, the total energy term, becomes $2E/(mR^2)$. Hence, we can make the identification $E = -Kc^2/(2m)$, or

$$E_K + U = E \propto -K .$$

5.4 Synopsis of matter-dominated solution

Under our assumption of a matter dominated universe, the analogy presented above can be related to the familiar classical mechanics problem of a mass

subject to a spherically symmetric gravitational field, for which $E = 0$ represents the dividing line between m being gravitationally bound or unbound. So we have:

- $K > 0 \Rightarrow E < 0 \Rightarrow$ “bound” (“closed”), R returns to 0.
- $K < 0 \Rightarrow E > 0 \Rightarrow$ “unbound” (“open”), R goes to infinity.
- $K = 0$ (“flat”) $\Rightarrow E = 0 \Rightarrow R \rightarrow \infty$ and $\dot{R} \rightarrow 0$ as $t \rightarrow \infty$.

These solutions for $R(t)$ as a function of t are summarized in Figure 12. The last solution, for a flat universe, corresponds in our analog to the solution for the classical escape velocity, where the velocity of the test mass goes to zero at infinity. We note that $K = 0$ is quite strongly favored by current observations. We also note that in this case, the condition $E = 0$ means that two large numbers K and U , the total kinetic and potential energies of the universe, have to cancel to large precision. We will discuss this seemingly unlikely situation when we discuss “inflation.”

It is interesting to evaluate the time evolution of the three cases above. For $K = 0$, it is easy to show that the Friedmann equation with $\rho = M/(4\pi R^3/3)$ becomes $R^{1/2}dR = \sqrt{2GM} dt$, which gives

$$R \propto t^{2/3}$$

and the age of the universe as $2/(3H_o)$. Furthermore, the *critical density* which enables this $E = 0$ solution (see homework) can straightforwardly be shown to be

$$\rho_c = \frac{3H_o^2}{8\pi G}. \quad (28)$$

For $K > 0$, one can show using a similar analysis that a “big crunch” occurs at a time $2\pi GM/c^3 \sim 10$ Gyr after the big bang.

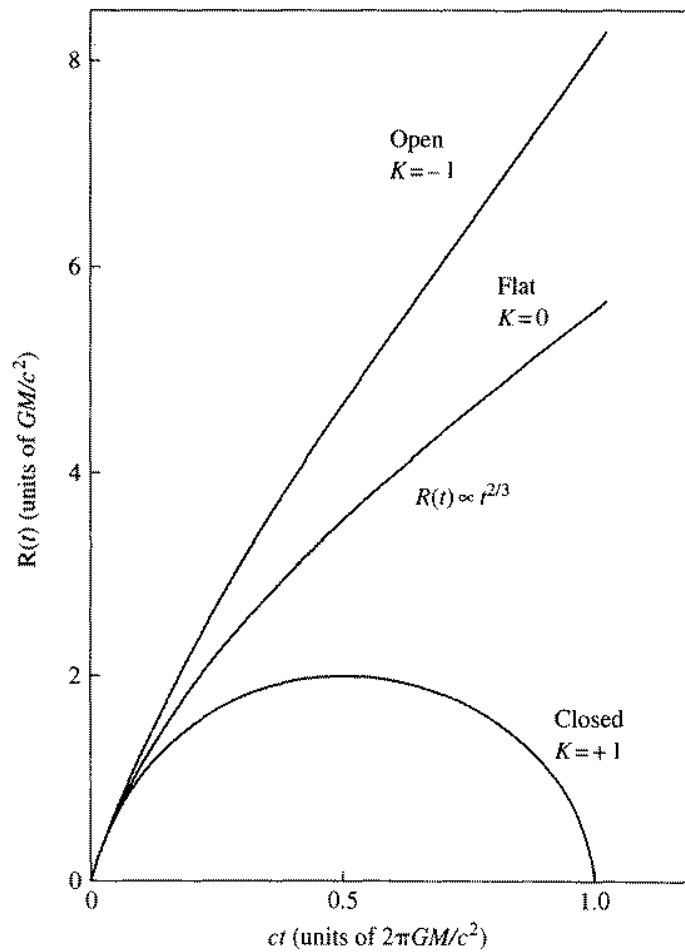


Figure 12: Time evolution of the scale parameter for the three possible types of spacetime curvature, K , assuming non-relativistic matter dominates the energy density.

6 Energy densities

We begin with a brief overview of the energy density contributions to the cosmological evolution of spacetime. Using our definition of the critical density in Eq. 28, $\rho_c = \frac{3H_0^2}{8\pi G}$, we can re-write the RHS of the Friedmann equation (Eq. 27):

$$H^2 = \left(\frac{8\pi G}{3}\right) \rho_{\text{tot}} - \frac{Kc^2}{R^2} = H^2 (\rho/\rho_c - 1) - \frac{Kc^2}{R^2},$$

or

$$\rho/\rho_c = \frac{Kc^2}{R^2 H^2} + 1. \quad (29)$$

Now, we define

$$\Omega \equiv \rho/\rho_c$$

and we write out the contributions to ρ due to (non-relativistic) matter, radiation (i.e. relativistic particles), and vacuum energy (see below):

$$\rho = \rho_m + \rho_r + \rho_v.$$

Finally, we divide through this expression by ρ_c to arrive at

$$1 = \Omega_m + \Omega_r + \Omega_v + \Omega_k, \quad (30)$$

where we have made the definition of an equivalent energy density due to spacetime curvature:

$$\Omega_k = -\frac{Kc^2}{R^2 H^2}.$$

Current observations of the present epoch give the following best values:

- $\Omega_k \approx 0$ (cosmic μ wave background observations, especially the most recent results from WMAP)
- $\Omega_r \approx 10^{-5}$
- $\Omega_m \approx 0.3$. All of normal (baryonic) matter is 0.05; the remainder is *dark matter*.
- $\Omega_v \approx 0.7$. This would be the contribution due to *dark energy* – more on this later.

Table 1: Properties of cosmic fluids

	$R(t)$	ρ	eqn. of state
matter	$R \propto t^{2/3}$	$\rho \propto R^{-3}$	$P = \frac{2}{3}\rho c^2 (v/c)^2$
radiation	$R \propto t^{1/2}$	$\rho \propto R^{-4}$	$P = \frac{1}{3}\rho c^2$
vacuum	$R \propto e^{\alpha t}$	$\rho = \text{const}$	$P = -\rho c^2$

The three types of cosmic fluids which we have input to our general relativistic description of matter and energy are listed in Table 1, along with a few of their important properties. The time-dependence $t^{2/3}$ for matter was determined in the previous section.

Figure 15 shows the cooling of the constituents due to cosmic expansion as a function of time, for the radiation and matter dominated eras. The transition between the radiation and matter eras occurs at the decoupling time, $t_{\text{dec}} \approx 3 \times 10^5 \text{ yr} \approx 10^{13} \text{ s}$. Before this time, photons, electrons, and protons were in thermal equilibrium, with

$$e^- + p \leftrightarrow H .$$

At t_{dec} , cooling has gone sufficiently below the ionization energy for hydrogen (13.6 eV) that the reaction above goes primarily from left to right, thus producing predominantly neutral matter which is “suddenly” transparent to photons. These photons are what we currently observe as the cosmic microwave background (CMBR) with a blackbody temperature of 2.7 K. This cooling corresponds to a redshift in the wavelength of 1100. So the decoupling time is:

$$t_{\text{dec}} = 3 \times 10^5 \text{ yr}; \quad (1 + z_{\text{dec}}) = 1100 \quad (31)$$

This last relation implies that the size of the universe was about 10^3 smaller at decoupling than today.

Finally, a useful relation is that between R and T :

$$R \propto 1/T . \quad (32)$$

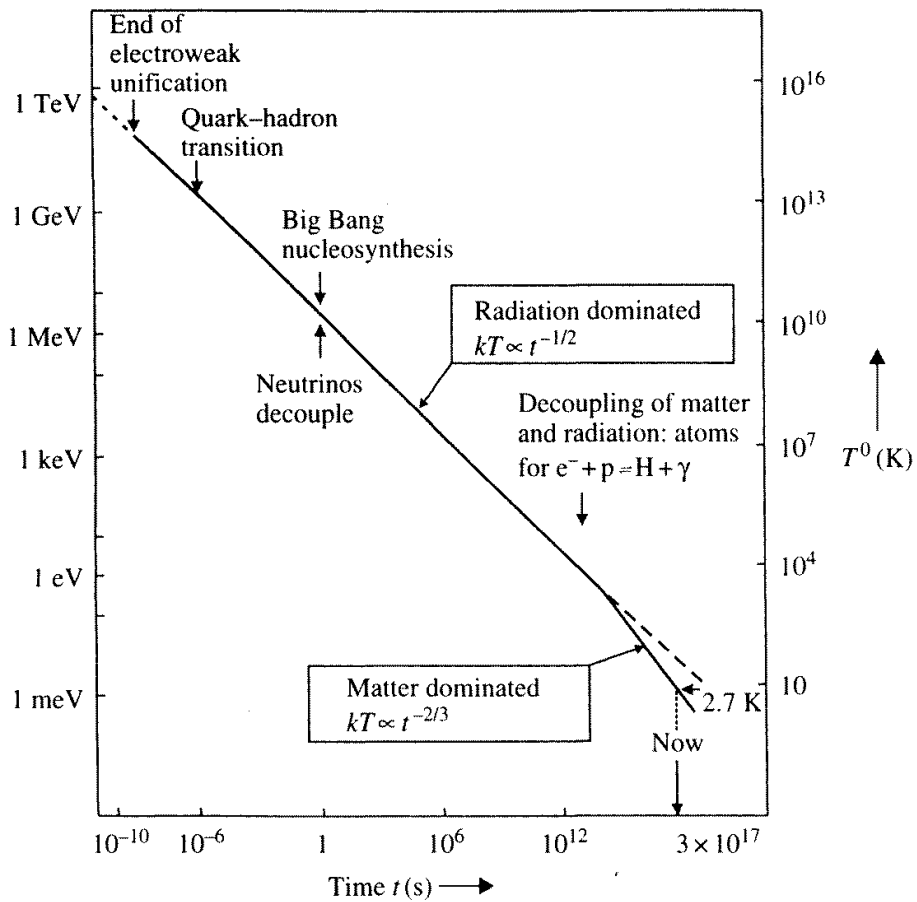


Figure 13: Energy (kT) per particle versus time. Radiation dominated the energy density until the time of photon decoupling, $t_{\text{dec}} \approx 10^{13}$ s.

7 Vacuum energy and Inflation

In Section 5 we introduced Einstein's field equations, Eq. 26, including the cosmological constant (Λ) term. Since $g_{\mu\nu}$ represents flat spacetime, this term is uniformly distributed. For the Friedmann equation, Eq. 27, this term gets included as $\Lambda/3$ on the RHS. Since this term has no R dependence, then for sufficiently large R , a non-zero Λ will eventually dominate the RHS of Eq. 27. In this case, the Friedmann equation becomes

$$\dot{R} = (\Lambda/3)R \Rightarrow \frac{dR}{R} = \sqrt{\Lambda/3} dt \Rightarrow R(t) \propto e^{\alpha t}, \quad (33)$$

where $\alpha \equiv \sqrt{\Lambda/3}$, as in Table 1.

Now, we make the connection between this funny Λ term in Einstein's equations and the idea of vacuum energy from quantum field theory (QFT). In quantum mechanics, the uncertainty principle states that there can be a non-conservation of energy ΔE over a time Δt such that

$$\Delta E \Delta t \geq \hbar/2 .$$

In QFT, this *must* occur with particle pairs such as e^+e^- appearing and disappearing, consistent with the uncertainty relation above. On average, there is a net contribution which is non-zero. This represents the *vacuum energy*. So the vacuum is not a state of nothing, it is simply the lowest energy level, or ground state. Hence, Einstein's general relativity will couple to this vacuum energy. In addition, in QFT we expect the vacuum to have a uniform energy density, just like the Λ field. Hence, we *identify vacuum energy with a non-zero Λ* . Hence, this allows us to possibly connect episodes of spacetime evolution influenced by Λ with fundamental elementary particles and fields. Such is the case for inflation, discussed below.

We complete the identification of Λ with vacuum energy by including it as a contribution to ρ in the Friedmann equation:

$$\rho_v = \frac{\Lambda}{8\pi G} .$$

We used ρ_v in this form in the previous section. We will not get into specific particle physics manifestations for inflation. We will motivate it using the observations of the CMBR and then discuss the properties the inflationary era must possess.

7.1 The Horizon problem of the CMBR

Refer to Figure 14, which shows the main features of the major epochs, going back to very early times. From the CMBR observations, we have a very good measurement of t_{dec} and z_{dec} , as shown in Eq. 31. If we extrapolate this to earlier times, using the $t^{1/2}$ scaling appropriate for this relativistic phase, then we can see from Fig. 14 that the universe at t_{dec} is too big. A more precise way to see this is the “horizon problem,” discussed below.

The *horizon* is the distance over which two objects are *causally connected*, that is they can exchange energy. Since such processes occur at speed c or less, then in a static universe, the horizon distance is simply $L_H = ct$, where t is the age of the universe. In an expanding universe, L_H is somewhat increased. In general, for $R \propto t^n$, then

$$L_H = \frac{ct}{1 - n} .$$

So for the radiation era, $n = 1/2$, and $L_H = 2ct$. Therefore, at the decoupling time we can expect that regions of radius $2ct_{\text{dec}}$ were in causal contact, in thermal equilibrium, and so at uniform temperature. Outside this volume, the hot plasma had developed independently, and so there it should not be expected to be at the same temperature.

We can easily relate the L_H for the CMBR to an angular range for our current CMBR observations. Since the decoupling time, a volume containing a single causal horizon has expanded with the general cosmic expansion by a factor $1 + z_{\text{dec}}$. Since such a region under current observation is at a light distance of $c(t_o - t_{\text{dec}})$, where t_o is the present time, then one CMBR horizon subtends an angle for current observations of

$$\theta = \frac{2ct_{\text{dec}}(1 + z_{\text{dec}})}{c(t_o - t_{\text{dec}})} \approx 2^\circ . \quad (34)$$

On the contrary, the CMBR observations indicate a remarkably uniform temperature *over the entire sky* at the level of $\Delta T/T \approx 10^{-5}$. This departure from naive expectation is known as the *horizon problem*. It must have been the case that our currently observable universe was entirely within one horizon at some early time. However, during the radiation era, $R \propto t^{1/2}$, whereas $L_H \propto t$, thus it is not easy to see how to make $R \sim L_H$ at some early time without some period of rapid expansion of R . Indeed, that is now thought to be the case. This period of rapid increase is known as *inflation*.

7.2 Inflationary scenario

We saw above (Eq. 33) that in principle some kind of vacuum energy, if it dominates the total energy density, can drive spacetime into a period of exponential expansion. For various particle physics reasons, it is generally assumed that this inflationary period begins at $t \sim 10^{-34}$ s. In the usual scenario, a spin-zero particle moves from a local minimum to a global minimum (the “true” vacuum) at this time. Inflation terminates when the true vacuum is attained.

What is required for the inflationary period? Let us extrapolate back from the decoupling time to the inflationary era, throughout which we expect $R \propto t^{1/2}$. Now the current Hubble radius is about 10^{26} m, so that at decoupling, the size of the universe was this divided by $(1 + z_{\text{dec}})$ or about 10^3 . So then at 10^{-34} s the size was

$$10^{23}(10^{-34}/10^{12})^{1/2} \sim 1 \text{ m}$$

whereas the horizon was $L_H = 2ct \sim 10^{-26}$ m. Hence inflation must make up these 26 orders of magnitude so that horizon can become comparable to the size of the universe, thus providing a uniform CMBR.

So from $H = \dot{R}/R$ we get for the inflationary expansion ratio

$$R_2/R_1 = e^{H\Delta t} = 10^{26} ,$$

or $H\Delta t$ needs to be $26 \ln(10) = 60$. We can write this in terms of a vacuum energy density using the Friedmann equation:

$$H^2 = \left(\frac{8\pi G}{3} \right) \rho_v = H_o^2 (\rho_v/\rho_c) .$$

The basic scenario is as shown in Figure 14.

In addition to the horizon problem, inflation also provides a solution for the *flatness* problem. This is related to our observation that the total energy E of the universe is very nearly zero, requiring the cancellation of two large numbers ($\sim 10^{70}$ J), the kinetic and potential energies of the universe. Recall that $E = 0$ corresponds to $K = 0$. Now, the curvature term in the Friedmann equation is Kc^2/R^2 . Hence, inflation this contribution suddenly by a factor $(R_2/R_1)^2 \sim 10^{52}$. Hence, after inflation when ρ_v no longer dominates, then from Eq. 29 we see that the extreme flatness requires that

$$\Omega = \rho/\rho_c = 1 \pm 10^{-52} , \tag{35}$$

or, in other words, $\Omega = 1$ to 1 part in 10^{52} .

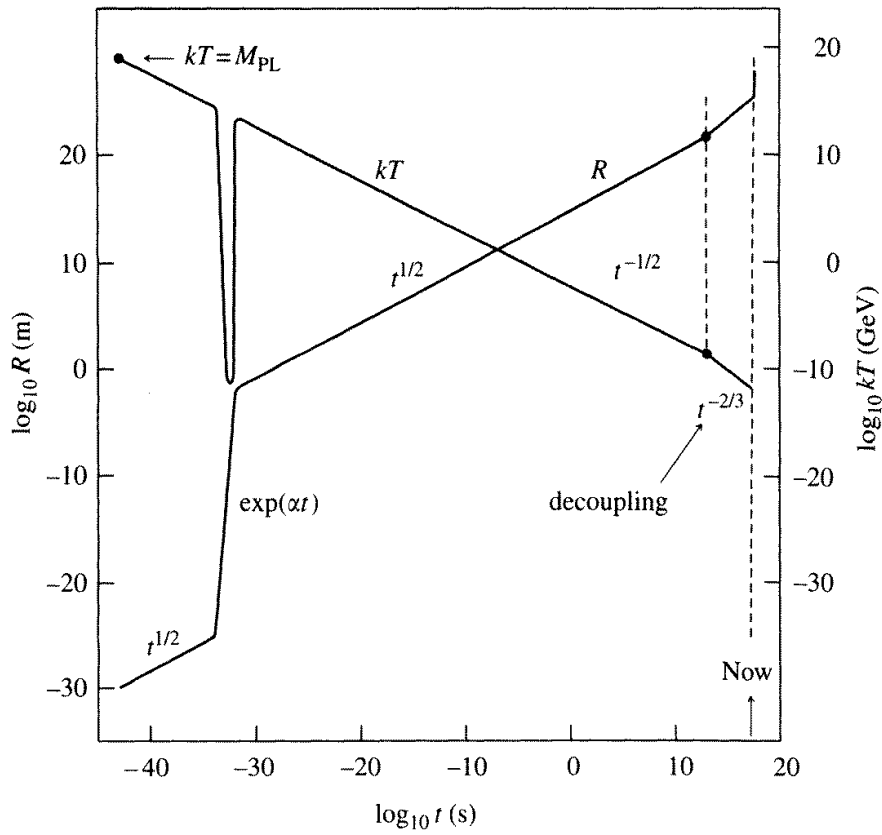


Figure 14: R and T vs time using expanded logarithmic scales. This shows the inflationary era at about $t = 10^{-34}$ s.

8 Fluids and 2nd Friedmann equation

Recall that we have discussed matter, radiation, and vacuum within the context of general relativity as ideal cosmic fluids. Along these lines, we now come up with a second relation for the time evolution of R which is also very useful.

Our ideal fluid obeys conservation of energy in the form of the First Law of Thermodynamics for an isolated system (no heat flow):

$$dE = -PdV ,$$

where E is the internal energy. Letting ρc^2 be the total energy density, then this becomes

$$d(\rho c^2 R^3) = -Pd(R^3) .$$

After carrying out the variations with respect to time and some algebra, we can solve for $d\rho/dt$:

$$\dot{\rho} = -3 \left(\frac{\rho c^2 + P}{R c^2} \right) \dot{R} . \quad (36)$$

If we now differentiate both sides of the Friedmann equation (Eq. 27) with respect to time, this gives

$$2\dot{R}\ddot{R} = \left(\frac{8\pi G}{3} \right) [R^2\dot{\rho} + 2\rho R\dot{R}] .$$

If we substitute for $\dot{\rho}$ from Eq. 36, this gives the so-called second Friedmann equation:

$$\ddot{R} = \left(\frac{4\pi GR}{3} \right) [\rho + 3P/c^2] . \quad (37)$$

A number of consequences spring from this result. First, for positive values of ρ and P , then $\dot{R} > 0$ immediately implies that $R = 0$ at some early time (the big bang). Next, we can use the equations of state for the fluid components from Table 1 to determine the resulting acceleration of the scale factor. Einstein's original idea for using Λ was to make $\rho + 3P/c^2 = 0$, which is possible since Λ gives a negative pressure. Note that in general, however, the equation of state for vacuum energy guarantees in fact that $\rho + 3P/c^2 < 0$, resulting in positive acceleration. This must have been the case for the inflationary period, and, according to recent evidence, we may just now be entering a new phase of positive acceleration due to the dominance of vacuum energy. This will be a topic of discussion in upcoming lectures.

9 Particle dark matter

We discuss some issues surrounding neutrinos as potential sources of dark matter. Although we will reject this hypothesis, neutrinos represent a prototype for other possible sources of particle dark matter, generically known as WIMPs. We will then discuss some possibilities for WIMPs and finish with some the difficult task of detecting WIMPs.

9.1 Neutrino decoupling

Figure 15 was also shown earlier in an earlier lecture. In this case we highlight the point at which neutrino decoupling occurs. Figure 16 gives another history of the universe, showing the main quantities of interest as powers of ten. At times prior to decoupling, the neutrinos are in equilibrium with the rest of the particle and radiation of the expanding universe according to equilibrium reactions such as

$$\gamma \leftrightarrow e^+e^- \leftrightarrow Z^0 \leftrightarrow \nu\bar{\nu} ,$$

where γ is a photon and the Z^0 particle is the neutral carrier of the weak interaction (see the particle physics primer). The large mass of the Z^0 (about $91 \text{ GeV}/c^2$) accounts for the short range of the weak interaction. Since neutrinos only couple to the weak force, they cannot directly interact with photons. As long as the neutrinos are frequently exchanging energy in reactions like this, then they will remain in thermal equilibrium. As the universe expands and cools, at some point the particles will no longer stay in thermal contact – this is decoupling. We encountered this earlier in the discussion of the decoupling of photons, thus giving rise to the cosmic microwave background. We now try to determine the point of decoupling.

We can use a simple relation to understand the point where decoupling occurs. As discussed previously, the particle collision rate is given by $\Gamma = n\sigma v$, where n is the particle density of the interacting particles, σ is the interaction cross section, and v is the relative speed of the colliding particles. We simply compare this collision rate with the rate of expansion of the universe, which is $H = \dot{R}/R$. So within factors of order 1, we find:

$$\Gamma = n\sigma v > H \Rightarrow \text{equilibrium} ; \quad (38)$$

$$\Gamma = n\sigma v < H \Rightarrow \text{decoupling} . \quad (39)$$

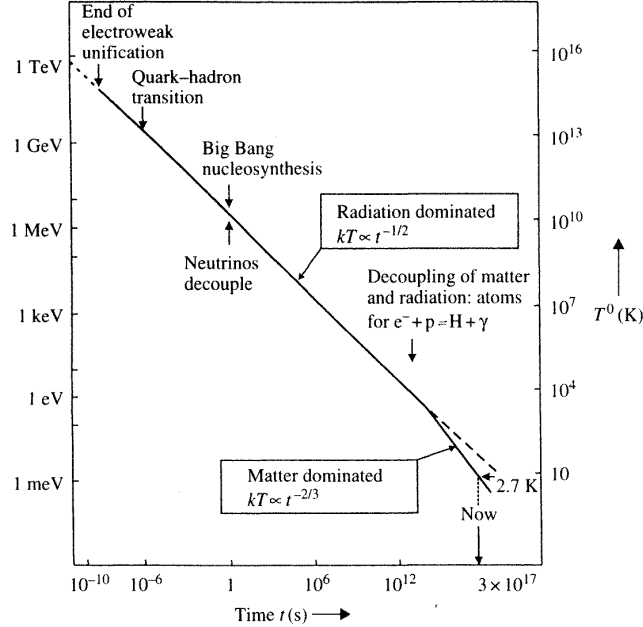


Figure 15: Energy (kT) per particle versus time. Note the indicated time of neutrino decoupling.

We can now input the known physics to determine the factors above. When we do, we find that $\Gamma = H$ at $kT \approx 1$ MeV, when the age of the universe was approximately 1 s.

9.2 Cosmic neutrino background

In class, we simply looked at the temperature dependence of each term of Eqs. 38-39 to determine that

$$\Gamma/H \propto T^3. \quad (40)$$

So the temperature of decoupling varies rapidly with collision rate, for example. We can use these ideas to qualitatively see how neutrino decoupling influenced formation of light nuclei, which began occurring slightly later, when $t \approx 1$ hr. Since we saw earlier that $H \propto g_*^{1/2} T^2$, where g_* increases with the number of available particle species, then a larger number of neutrino types,

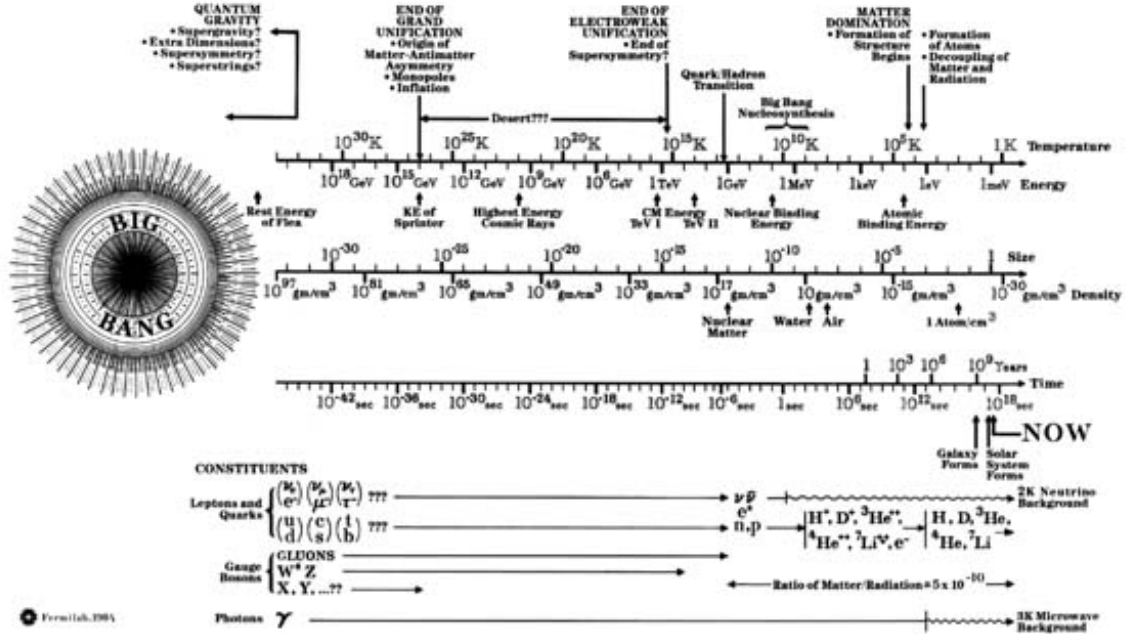


Figure 16: Logarithmic history of the universe.

N_ν , increases H and therefore, by Eq. 40, the decoupling temperature increases (decoupling occurs earlier). This in turn means that the equilibrium ratio of neutron to proton density,

$$n/p = e^{-Q/kT} ,$$

where $Q = (m_n - m_p)c^2 = 1.3 \text{ MeV}$, is larger at decoupling. The larger n/p ratio then implies a larger fraction of neutron-rich nuclei. In particular, a larger N_ν gives rise to a predicted ${}^4\text{He}/H$ ratio which is larger.

The quantitative versions of the above arguments were used in the 1980's to predict the number of neutrino species in nature to be about $N_\nu \leq 4$ based on the observed nuclei ratios. Subsequently, in 1989, accelerator experiments were able to measure N_ν accurately. The method used was to produce the Z^0 particle in the process $e^+ + e^- \rightarrow Z^0$. This produces a resonance when the collision energy is equal to the mass of the $Z^0 \approx 91 \text{ GeV}/c^2$, as shown in Fig. 17. The width of this quantum state depends on the number of possible

decay modes, and hence N_ν . The current experimental result is

$$N_\nu = 3.00 \pm 0.01 .$$

Hence the prediction based on cosmic astrophysics was confirmed.

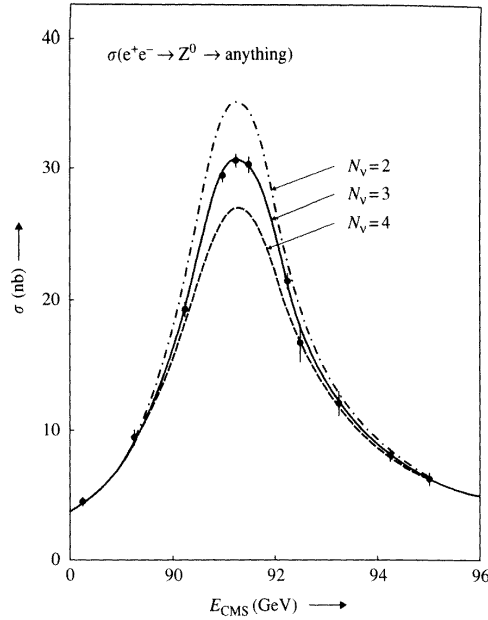


Figure 17: Accelerator experiment result showing the excitation of the Z^0 resonance. The curves show the theoretical expectations for different assumptions for the number of neutrino species.

The neutrinos which decoupled from the cosmic fireball at $t \approx 1$ s, in analogy to the 2.73 K photon background, should still be around. As discussed in the previous lecture, the predictions are that the density of these neutrinos is

$$n_\nu = 113 \times N_\nu \approx 340 \text{ cm}^{-3} ,$$

with an average thermal temperature now of 1.95 K.

9.3 Neutrinos as dark matter

We saw in Lecture 7 that there is now good evidence that all 3 neutrino species have a small, but finite, rest mass, $m_\nu \sim 10^{-3} \text{ eV}/c^2$. But since there

are a lot of them around us from the decoupling, then perhaps this gives an appreciable contribution to the estimated dark matter mass density. We find that to make a critical density from cosmic neutrinos requires that the mass of the 3 species total $47 \text{ eV}/c^2$, that is

$$\rho_\nu = \rho_c \Rightarrow \rho_\nu = 340 \times 47 \text{ eV}/\text{cm}^3. \quad (41)$$

We would require about 30% of this in order for neutrinos to give the “right” contribution to dark matter. The data suggests it is about 10^3 short of this. So it seems that neutrinos contribute rather insignificantly to dark matter.

There is one other reason why it was not expected that neutrinos would contribute to this. Structure formation (companion lecture) demands that the dark matter be “cold,” that is, that the particles be non-relativistic during the early era of structure formation. Recall that the neutrinos decouple with an average energy $kT \approx 1 \text{ MeV}$, much larger than the rest energies. Indeed, at the dawn of structure formation, the neutrinos would have only cooled to $\sim 10 \text{ eV}$, still relativistic. Therefore, neutrinos are not only too light, but also too “hot” to be an important contributor to dark matter.

9.4 WIMPs

We didn’t discuss this in much depth in class. But this is an important topic for both astrophysics/cosmology and elementary particle physics (aka HEP). An important issue in HEP theory is that basic calculations become untenable at energies which are about 10 times higher than the reach of our current accelerators, which currently probe elementary particle interactions at energies of $\sim 200 \text{ GeV}$. One solution to this is a theory called *supersymmetry*, aka SUSY. A prediction of SUSY is that there is a stable, neutral, weakly interacting particle, usually called the neutralino, χ^0 . For our present purpose we can simply think of these as heavy neutrinos. Generically, such dark matter candidates are called WIMPs, for weakly-interacting massive particle.

Just as with neutrinos, we can evaluate WIMP decoupling using Eqs. 37 and 38. However, because they are massive, they will be non-relativistic at decoupling, and hence will contribute to cold dark matter (CDM). The decoupling temperature is about $Mc^2/kT \approx 25 \pm 5$ for a WIMP of mass M . The WIMP energy distribution will follow a Boltzmann function after decoupling. Generically, the WIMP energy density is found to follow

$$\rho_{\text{wimp}}/\rho_c \sim [10^{-25} \text{ cm}^3\text{s}^{-1}] / (\sigma v).$$

Figure 18 gives this critical density as a function of WIMP mass M , basically reflecting the denominator in the equation above. Qualitatively, we see three branches in this figure. The first, at low mass, corresponds to light, relativistic WIMPs. Neutrinos fall on this branch, but off scale at low mass. The next branch, at intermediate mass, is for WIMPs which are non-relativistic at decoupling. For these masses, the weak cross section varies as $\sigma \propto G_F^2 M^2$. The form of the weak cross section changes for masses near the mass of the weak force quanta, the W and Z^0 particles, which have masses of about 90 GeV/c², to

$$\sigma \propto G_F^2 \left[\frac{M^2}{(M^2 + M_Z^2)^2} \right] ,$$

which gives the third branch. The shaded region is the range of cosmological interest for dark matter. This third branch is the one where one would expect the SUSY particle.

9.5 WIMP detection

The best and clearest way to test the WIMP particle dark matter solution is to look at data from the next generation of particle accelerator, such as the LHC in Europe, and the proposed linear collider. These accelerators will probe exactly the energy range given by the intersection of the third branch and the shaded region in Fig. 18. The SUSY version of this solution would be that the WIMP be the neutralino, χ^0 . In the accelerator interactions, one could test if the observed WIMP had the right properties, including stability against decay, to be a real manifestation of cold dark matter.

On the other hand, one would also like to directly observe the relic WIMPs left over from cosmic decoupling. In an earlier lecture, we showed the difficulty of measuring neutrino interactions in accelerators. WIMP detection is even more challenging, since the kinetic energy, and hence the interaction rate with matter, is much, much smaller. A generic estimate for the rate (R) per unit detector mass for WIMP interactions in a detector utilizing a medium of atomic mass A is roughly

$$R \sim 10^4 / (AM) \text{ events/kg/day} ,$$

for a WIMP of mass M . This is experimentally *very* challenging.

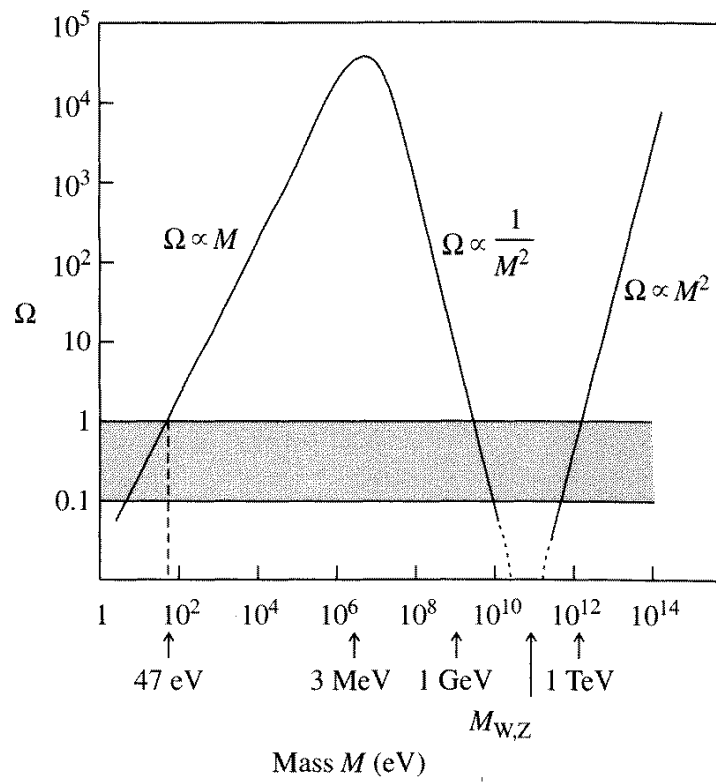


Figure 18: $\Omega_w = \rho_{\text{wimp}}/\rho_c$ vs WIMP mass (eV). From Perkins